Article

Cell Chemical Biology

A Multifunctional Monooxygenase XanO4 Catalyzes Xanthone Formation in Xantholipin Biosynthesis via a Cryptic Demethoxylation

Graphical Abstract

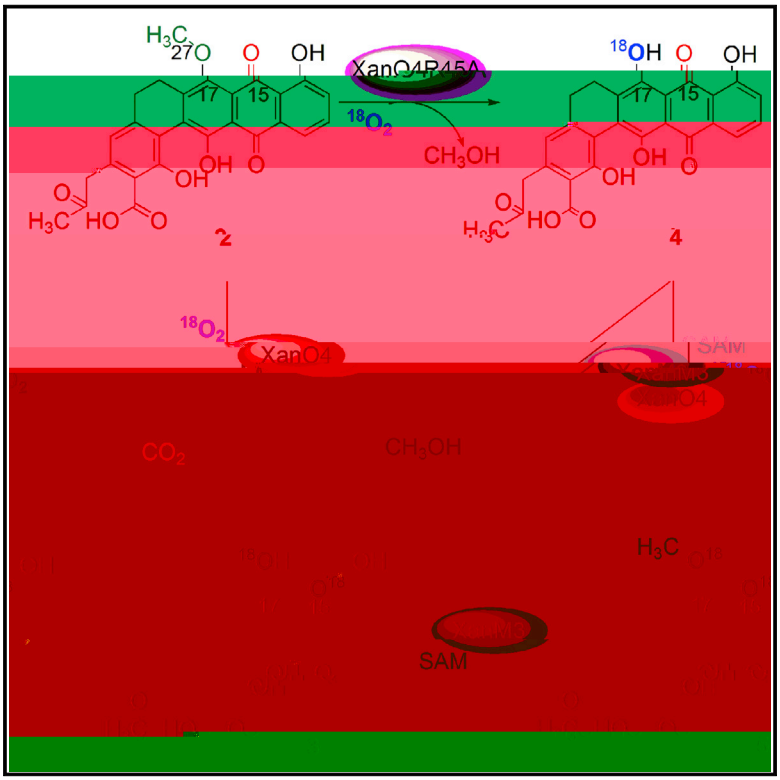

Authors

Lingxin Kong, Weike Zhang, Yit Heng Chooi, ..., Zixin Deng, Yiwen Chu, Delin You

Correspondence

dlyou@sjtu.edu.cn

In Brief

Kong et al. discovered an unusual multifunctional flavin-containing monooxygenase (FMO) XanO4 that transforms an anthraquinone intermediate to the xanthone system in xantholipin, a polycyclic xanthone antibiotic. The reaction is accompanied by a cryptic demethoxylation that is indispensable for xanthone formation. These findings expand the inventory of FMO-mediated reactions.

Highlights

- XanO4 is a multifunctional flavin-containing monooxygenase
- XanO4 catalyzes the oxidative transformation of anthraquinone to xanthone
- Cryptic demethoxylation is essential for the formation of a xanthone ring
- XanO4-mediated reaction is general in polycyclic xanthone antibiotics

Accession Numbers

ADE22300.1
ADE22301.1
AHX24715.1
CAM34363.1

Kong et al., 2016, Cell Chemical Biology *23*, 508–516
April 21, 2016
http://dx.doi.org/10.1016/j.chembiol.2016.03.013

Please cite this article as: Kong et al., A Multifunctional Monooxygenase XanO4 Catalyzes Xanthone Formation in Xantholipin Biosynthesis via a Cryptic Demethoxylation, Cell Chemical Biology (2016), http://dx.doi.org/10.1016/j.chembiol.2016.03.013

A Multifunctional Monooxygenase XanO4 Catalyzes Xanthone Formation in Xantholipin Biosynthesis via a Cryptic Demethoxylation

Lingxin Kong,[1] Weike Zhang,[1] Yit Heng Chooi,[2] Lu Wang,[3] Bo Cao,[1] Zixin Deng,[1] Yiwen Chu,[3] and Delin You[1,4,*]
[1]State Key Laboratory of Microbial Metabolism, School of Life Sciences & Biotechnology, Shanghai Jiao Tong University, Shanghai 200240, China
[2]School of Chemistry and Biochemistry, University of Western Australia, Perth, WA 6009, Australia
[3]Sichuan Industrial Institute of Antibiotics, Chengdu University, Chengdu 610052, China
[4]Joint International Research Laboratory of Metabolic and Developmental Sciences, Shanghai Jiao Tong University, Shanghai 200240, China
*Correspondence: dlyou@sjtu.edu.cn
http://dx.doi.org/10.1016/j.chembiol.2016.03.013

SUMMARY

Xantholipin and several related polycyclic xanthone antibiotics feature a unique xanthone ring nucleus within a highly oxygenated, angular, fused hexacyclic system. In this study, we demonstrated that a flavin-dependent monooxygenase (FMO) XanO4 catalyzes the oxidative transformation of an anthraquinone to a xanthone system during the biosynthesis of xantholipin. In vitro isotopic labeling experiments showed that the reaction involves sequential insertion of two oxygen atoms, accompanied by an unexpected cryptic demethoxylation reaction. Moreover, characterizations of homologous FMOs of XanO4 suggested the generality of the XanO4-like-mediated reaction for the assembly of a xanthone ring in the biosynthesis of polycyclic xanthone antibiotics. These findings not only expand the repertoire of FMO activities but also reveal a novel mechanism for xanthone ring formation.

INTRODUCTION

Microbial polycyclic xanthone antibiotics (Figures 1A and S1), including xantholipin (**1**), lysolipin, FD-594, and arixanthomycin, are a subgroup of natural polyketide products, characterized by a highly oxygenated, angular, fused hexacyclic skeleton with a unique xanthone ring nucleus (marked in red in Figure 1) (Winter et al., 2013; Kang and Brady, 2014). Since the isolation of the first member albofungin over 40 years ago, this novel class of molecules has attracted noticeable attention from both the synthetic and biological communities due to their attractive chemical structures and diverse biological activities, such as antibacterial activities (mainly Gram-positive bacteria), antifungal activities, antitumor activities, and anticoccidial activities (Winter et al., 2013; Sloman et al., 2011; Masuo et al., 2009; Butler et al., 2011; Yang et al., 2015). Xantholipin, isolated from the culture broth of *S* in 2003 (Terui et al., 2003), possesses strong antibiotic activity against several Gram-positive bacteria and potent cytotoxicity activity against the leukemia cell line HL60 and the oral squamous carcinoma cell line KB (Zhang et al., 2012). Xantholipin showed an inhibitory effect on heat-shock protein 47 (HSP47) (half maximal inhibitory concentration [IC_{50}] <0.2 μM) and was recently identified as a lead drug for the treatment of fibrotic diseases with an IC_{50} value of 27 nM for inhibition of collagen production. The biological activities of this class of compounds are associated with their privileged xanthone ring nucleus (Zhang et al., 2012; Pinto et al., 2005; Masters and Bräse, 2012). Hence, elucidation of the biosynthesis of the xanthone ring in **1** can provide a foundation for combinatorial biosynthesis of polycyclic xanthone antibiotics.

Previous biosynthetic studies of polycyclic xanthone antibiotics, such as **1** (Zhang et al., 2012), lysolipin (Lopez et al., 2010), FD-594 (Kudo et al., 2011), and arixanthomycin (Kang and Brady, 2014) have demonstrated that these molecular backbones are derived from a single polyketide chain, which was synthesized by a type II polyketide (iterative) synthase (PKS). During screening for the enzyme responsible for the xanthone ring formation in **1**, we focused our research on a flavin-dependent monooxygenases (FMO) XanO4. XanO4 contains a monooxygenase (Pfam01360) and a flavin adenine dinucleotide (FAD)-binding (Pfam01494) conserved domain (Figure S2A). It exhibits significant homology to known bacterial class A FMOs involved in the Baeyer-Villiger (BV) oxidation reaction, such as MtmOIV (30% identity) and GrhO5 (42% identity) in mithramycin (Gibson et al., 2005) and griseorhodin (Yunt et al., 2009) biosynthesis, respectively. Deletion of *O4* abolished the production of **1** and led to the accumulation of a red pradimicin-type anthraquinone intermediate **2**, which is a methoxylated anthraquinone (Figure 1B) based on previous structural analysis (Zhang et al., 2012). These results suggested that XanO4 is the candidate enzyme required for the conversion of the anthraquinones **2** into a xanthone, presumably via BV oxidation.

RESULTS

In Vitro Reconstitution of the Xanthone Ring

To determine whether XanO4 is directly involved in xanthone formation from **2**, we cloned *O4* and expressed it in *E*

BL21 (DE3). The recombinant XanO4 was purified as a brightly yellow protein, suggesting the existence of a prosthetic group. The purity and size (62 kDa) of the protein were

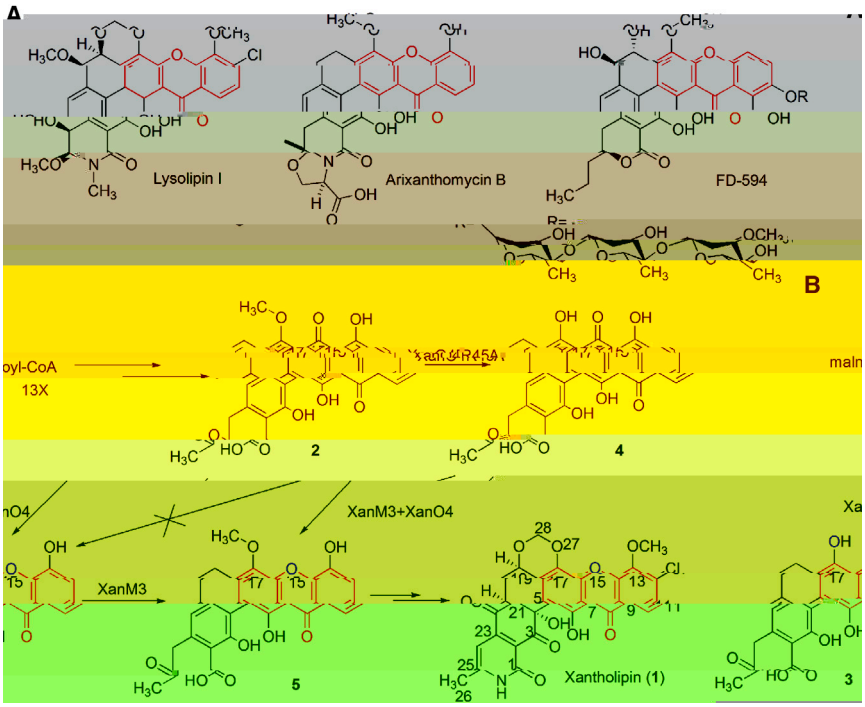

Figure 1. Chemical Structures and Biosynthetic Routes

(A) Structures of other natural polycylic xanthone antibiotics.

(B) The proposed biosynthetic pathway of the xanthone ring in xantholipin. The xanthone ring is shown in red with the oxygen atom originating in the xanthone ring marked in blue. For related polycyclic xanthone antibiotics, see Figure S1.

determined by SDS-PAGE, shown in Figure S2B. High-performance liquid chromatography (HPLC)-mass spectrometry (MS) analysis of the supernatant of denatured XanO4 proved the presence of FAD cofactor (Figures S2C and S2D). FAD could be reduced by XanO4 with either NADH or NADPH (Figure S2E). XanO4 was added into an in vitro assay system in the presence of NADPH and FAD, using intermediate **2** as substrate. After 30 min of incubation at 30°C, XanO4 was able to catalyze the conversion of **2** into a new product **3** (Figure 2A). Time-course analysis detected a decrease of **2** over time with a concurrent increase of **3** (Figure 2B). LC-MS analysis of **3** gave molecular ion peaks at / 461.4 ($[M - H]^-$) (Figure S3D), 26 Da less than that of compound **2** ($C_{27}H_{20}O_9$, / 487.1 $[M - H]^-$) (Figure S3A), indicating the two carbon atoms and two hydrogen atoms missing from **2**. The characteristic UV-vis absorption with λ_{max} at 405 nm of **3** (Figure S3D) indicated its intrinsic chromophore had changed from **2**. High-resolution electrospray ionization (ESI)-MS analysis revealed the molecular formula $C_{25}H_{18}O_9$ (calcd. 461.0951, found 461.0877 $[M - H]^-$; Figure S3D). We then scaled up the above enzymatic reactions and purified compound **3** by preparative HPLC (see Experimental Procedures). ^1H and ^{13}C nuclear magnetic resonance (NMR) spectra data analysis revealed that **3** is a pentacyclic demethyl-naphthaxanthone intermediate (Figure 1B and Table S3), in which an oxygen atom (O15) has replaced the C15 carbonyl group of **2** (C15), forming a xanthone system (Figure 1B). These data confirmed that XanO4 is the monooxygenase responsible for the formation of the xanthone ring in **1**.

Oxidative Demethoxylation Reaction Coupled with Xanthone Ring Formation

The above structural analysis revealing the absence of the methyl group at the hydroxyl group of C17 in **3** (Table S3) was puzzling, and suggested that the oxidative transformation of anthraquinone **2** to xanthone **3** by XanO4 was accompanied by a demethylation. Given that most demethylases share a common mechanism via hydroxylation of the N- or C-methyl moiety to give a hemiaminal intermediate followed by spontaneous elimination of the methyl group in the form of formaldehyde (Klose et al., 2006), we first tested this possible leaving group by detecting the hydroxymethane sulfonate adduct (HMS^-, $CH_2(OH)SO_3^-$) resulting from the reaction of formaldehyde with sodium bisulfate (Jiang et al., 2013) (Figure S4A). However, no mass signal corresponding to / 111 ($[M - H]^-$) for HMS^- was found in the reaction system (Figure S4D). Next, we proposed that oxidative replacement of the C17 methoxy group with a hydroxyl group newly derived from molecular oxygen may occur. When $^{18}O_2$ was used to replace $^{16}O_2$ in the in vitro enzymatic reaction systems, MS analysis of the reaction mixtures revealed an increase in mass of 2 and 4 Da for **3**, confirming the incorporation of one and two labeled oxygen atoms, respectively (Figure 3). The incorporation of two oxygen atoms is surprising. The results indicated that besides the expected incorporation of oxygen in the xanthone core, another oxygen atom derived from molecular oxygen was inserted at C17 during the construction of the xanthone ring and the C17 methoxy group was likely disposed of in the form of methanol. The observation of **3** with a single labeled oxygen atom incorporated (Figure 3) is likely attributed to incomplete depletion of $^{16}O_2$ as we showed that the oxygen atom from H_2O^{18} was not incorporated into **3** (Figure S4F).

Methoxy Group of C17 in 2 Is Essential for Xanthone Ring Construction

Considering the existence of a methylene carbon atom C28 in the methylenedioxy-bridge structural moiety of **1** (Figure 1B), the methyl group of hydroxyl group at C17 may play an important role in the biosynthesis of xantholipin. Multiple sequence alignment of XanO4 and XanO4 homologs with MtmOIV suggested a conserved arginine residue R45 corresponds to R52 in MtmOIV (Figure S2A), which has been suggested to be important for FAD binding and the BV oxidation reaction in mithramycin biosynthesis (Beam et al., 2009). We next performed a point mutation R45A on XanO4. Incubation of the XanO4-R45A mutant with **2** did not result in the production of **3** but yielded another new product **4** upon prolonged incubation overnight (Figure 4A).

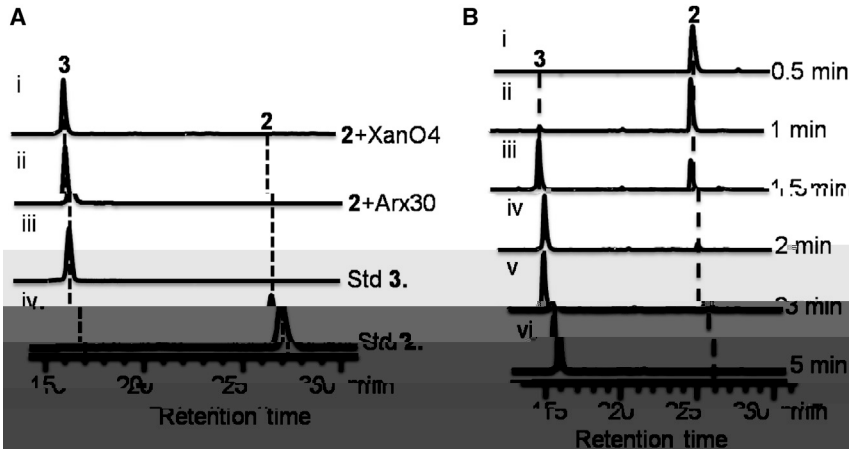

Figure 2. In Vitro Reconstitution of the Xanthone Ring Catalyzed by XanO4

(A) HPLC profiles of (i) XanO4 incubated with **2**; (ii) Arx30 incubated with **2**; (iii) standard **3**; (iv) standard **2**.

(B) Time course of production of **3** catalyzed by XanO4. 20 μM XanO4 was incubated with 50 μM compound **2** for (i) 0.5 min; (ii) 1 min; (iii) 1.5 min; (iv) 2 min; (v) 3 min; (vi) 5 min. Enzymatic characterization of XanO4 is shown in Figure S2; mass and high-resolution electrospray ionization-MS analyses are given in Figure S3.

MS analysis of **4** (Figure S3B) gave a molecular ion peak at / 473.4 $[M - H]^-$, 14 Da less than that of **2**, corresponding to the loss of CH_2. The UV-vis spectrum (Figure S3B) and comparison of the structure signals in ^{1}H-NMR at C17 and ^{13}C-NMR at C15 (Figure S3C) supported that **4** retained the anthraquinone structure and is the demethylated derivative of **2**. Thus, R45 is essential for the BV oxidation catalyzed by XanO4, but the R45A mutant retained a small amount of demethoxylation activity. Insertion of an oxygen atom from molecular oxygen at C17 can be observed in an in vitro assay of XanO4R45A and **2** with $^{18}O_2$, confirming the demethoxylation reaction (Figure 4B).

The isolation of **4** allowed us to investigate if the methoxy group at C17 is indispensable for the oxidative transformation of **2** to **3**. Interestingly, assaying XanO4 with **4** resulted in no new product (Figure 4C), even after extended incubation. This suggests that the demethoxylation reaction is essential for the conversion of the anthraquinone system in **2** to xanthone **3**. Finally, we showed that XanM3, one of the three methyltransferases encoded in the gene cluster, can remethylate **4** to **2** (Figure 4C). In a one-pot reaction with XanM3 and XanO4, the two enzymes were able to convert **2** to a new product **5** (Figure 4C). The retention time, UV-vis spectrum, and MS data of this new product is consistent with the dechlorinated naphthaxanthone intermediate **5** from Δ *H* mutant (Figures 1, S3E, and S5). The structure of **5** was confirmed as the O-methylated derivative of **3** by extensive NMR analysis (Table S3). Together, these data showed that an essential cryptic demethoxylation step was involved in the oxidative transformation of the anthraquinone intermediate to the final xanthone scaffold in **1**. The demethoxylation reaction was masked by the re-methylation of C17 by the methyltransferase XanM3, which can act on both anthraquinone and xanthone scaffolds.

Generality of XanO4-Mediated Xanthone Ring Formation in Polycyclic Xanthone Antibiotics

Phylogenetic analysis showed that XanO4 clustered into the same clade with MtmOIV and GrhO5, suggesting that it is a member of type O BV monooxygenases (belongs to class A FMOs), which lack the typical sequence motif of type I BVMOs and are not related to type II BVMOs (Figure 5) (Leisch et al., 2011). XanO4 further formed a small well-supported subclade with FMOs from other polycyclic xanthone pathways, including Arx30 of the arixanthomycin pathway, LlpOVIII of the lysolipin pathway, and PnxO4 from the FD-594 pathway. This suggests that these FMOs may use the same strategy in the biosynthesis of other polycyclic xanthone antibiotics. Interestingly, an O-methyl group at the position corresponding to C17 on **1** can be found in the intermediates or final products of lysolipin, arixanthomycin, FD-594, and other structurally related polycyclic xanthone pathways (Figures 1A and S1). To evaluate the generality of this novel FMO-mediated anthraquinone to xanthone transformation, two homologous genes of *O4* were cloned. Genes for Arx30 (60% identity to XanO4) and LlpOVIII (70% identity to XanO4) from a metagenome library (Kang and Brady, 2014) and *S* (Lopez et al., 2010), respectively, together with *O4*, were introduced individually into Δ *O4* mutants. All the complementation and -complementation strains partially restored the production of **1** (Figure S6). For further verification, recombinant Arx30 was expressed and purified for an in vitro assay with **2**. Similarly, Arx30 could catalyze the conversion of **2** into **3** (Figure 2A). The genetic and biochemical characterizations of XanO4 homologs suggested that the same strategy involving a cryptic demethoxylation is employed in the biosynthesis of related polycyclic xanthone antibiotics.

DISCUSSION

Sequence analysis of XanO4 obviously pinpointed XanO4 as a member of class A FMOs (see Figure S2A), which mainly catalyze hydroxylations. Previous isotopic labeled precursor feeding experiments have supported the single acetate/malonate-derived polyketide molecular frameworks with interruptions at the xanthone ring (Carter et al., 1989, 1991; Bockholt et al., 1994; Kondo et al., 1998). In particular, the lysolipin isotope feeding study revealed the incorporation of two oxygen atoms into the positions corresponding to O15 and O27 in **1** (Figure 1B), which is in agreement with our results. Based on the incorporation into O15, the authors suggested that the biosynthesis of lysolipin involved BV oxidation followed by rearrangement to

XanO4 catalyzes oxidative replacement of the carbonyl group and methoxy group in anthraquinone compound **2** (see Figure 3B), resulting in xanthone ring formation and replacement of the methoxy with a hydroxyl group. The unexpected demethoxylation is likely facilitated by methanol as the leaving group. The C17 methoxy group has been shown to be indispensable for xanthone formation and the mutant XanO4-R45A catalyzed the demethoxylation reaction without xanthone formation. All of the aforementioned results contributed to the proposal of the mechanism for XanO4 (Figure 6), in which this multifunctional FMO first catalyzed the oxidation at C17, potentially via an epoxide intermediate. This resulted in breaking of the aromaticity of the ring and permitted the subsequent BV oxidation and ring cleavage. This is followed by decarboxylation, leaving of the C17 methoxy as methanol, and formation of the xanthone ring. This made the reaction a novel type different from the classic BV oxidation-mediated oxygen atom insertions reported recently (Gibson et al., 2005; Jiang et al., 2009; Tang et al., 2013; Hu et al., 2014) but reminiscent of the anthraquinone to xanthone conversion in fungi proposed by Henry and Townsend (2005), which involved an epoxidation that activate the anthraquinone for BV-type rearrangement. Similarly, we believed that C17 oxidation primes the anthraquinone **2** for BV oxidation and rearrangement, while the methoxy group also served as a better leaving group than hydroxyl and hence it is essential for xanthone formation. Nonetheless, it is intriguing that all these steps are accomplished by a single enzyme XanO4, while up to three enzymes have been proposed to be required for the con-

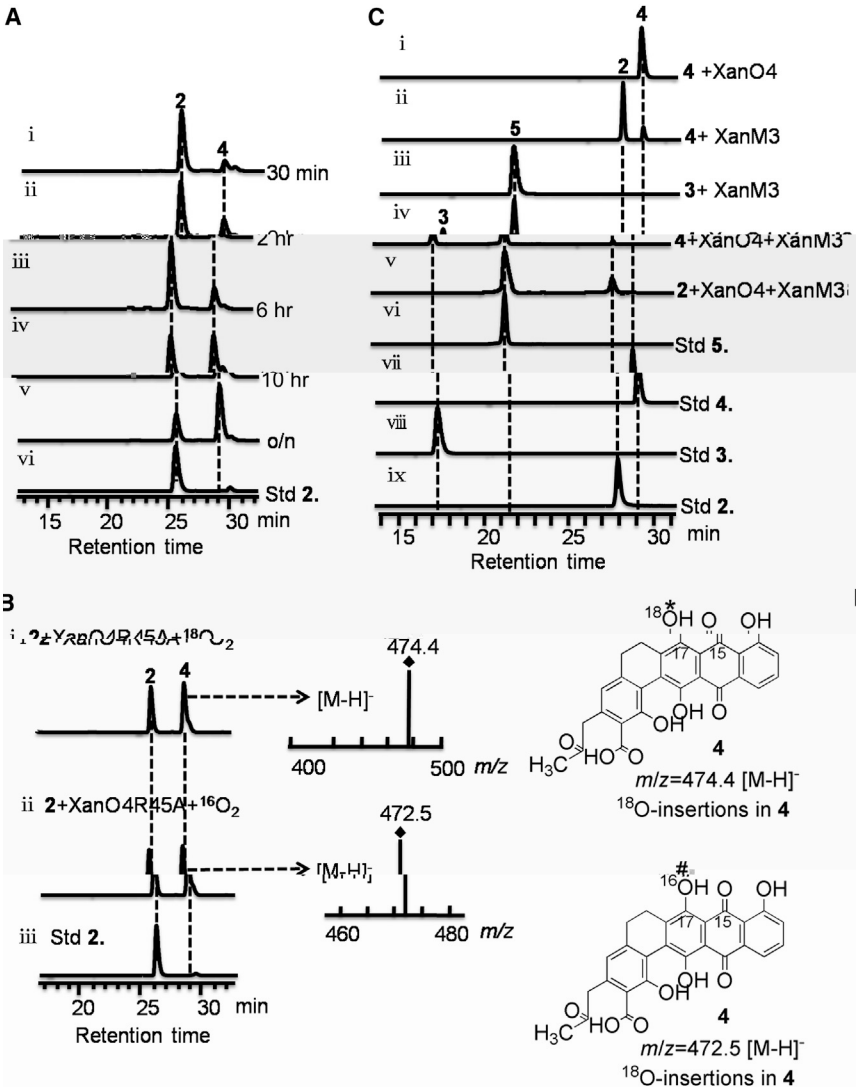

Figure 4. Cryptic Demethoxylation and Re-methylation Involved in Xantholipin Biosynthesis

(A) Time course of production of **4** catalyzed by XanO4R45A. 20 μM XanO4R45A was incubated with 50 μM compound **2** for (i) 30 min; (ii) 2 hr; (iii) 6 hr; (iv) 10 hr; (v) overnight; with standard **2** as control (vi).

(B) MS analysis of the product from **2** catalyzed by XanO4R45A (i) under $^{16}O_2$; (ii) under $^{18}O_2$; with standard **2** as control (iii). Oxygen atoms derived from $^{18}O_2$ and $^{16}O_2$ are marked with * and #, respectively.

(C) HPLC profiles of reactions of (i) compound **4** with XanO4; (ii) compound **4** with XanM3; (iii) compound **3** with XanM3; (iv) compound **4** with XanO4 and XanM3; (v) compound **2** with XanO4 and XanM3; (vi) standard **5**; (vii) standard **4**; (viii) standard **3**; (ix) standard **2**.

EXPERIMENTAL PROCEDURES

Strains and General Techniques for DNA Manipulations

Bacterial strains and plasmids used in this study are listed in Table S1.

S. SS101 (Terui et al., 2003), the wild-type producer of xantholipin, was used as the original strain for the construction of Δ*H* mutants. ZWK8, Δ*O4* mutant of *S.* SS101 (Zhang et al., 2012), was used for large-scale fermentation of compound **2**. *E. coli* BW25113/pKD46 was used for the standard procedure of gene replacement based on λ-Red-recombination (Datsenko and Wanner, 2000; Gust et al., 2003). *E. coli* DH10B was used for routine gene cloning. *E. coli* ET12567/pUZ8002 (Paget et al., 1999) was the nonmethylating plasmid donor strain for intergeneric conjugation with *S.* SS101. *E. coli* BL21(DE3)/pLysE was used as host for protein expression. pRSETb (Invitrogen) and pET28a (Novagen) were used as protein expression vectors. pIJ773 (Datsenko and Wanner, 2000; Gust et al., 2003) was used as the template for amplification of an *(3)IV + T* cassette for the disruption of *H*. pJTU1278 (He et al., 2010), the derivative plasmid of pHZ1358, was used for gene complementation. pMD18-T (TaKaRa) and pBlueScript II SK plus (Stratagene) were used for sequencing of DNA fragments. General procedures for *E. coli* or *S.* manipulation were carried out according to Kieser et al. (2000) and Sambrook and Russel (2001).

Plasmids Constructions

The primers used in this study are listed in Table S1.

Genomic DNA isolated from *S.* was used as the template for PCR amplification of *O4* and *M3*. The fidelity of *O4* and *M3* was confirmed by DNA sequencing. The gene *O4* was first recovered as NdeI and EcoRI fragments and was then inserted into the same sites of pET28a, leading to recombinant plasmid pKLX1. The gene *M3* was first recovered as BamHI and EcoRI fragments and was then inserted into the same sites of pRSETb, leading to recombinant plasmid pKLX2. pIJ773, digested with HindIII and EcoRI, was used as the template for PCR amplification of the 1.4 kb gene disruption *(3)IV + T* cassette (Apr^R gene) using pair of primers *H*tarf- *H*tarr. The resultant fragment was electrotransformed into *E. coli* BW25113/fosmid 22E4 for replacement of the 800 bp of *H*. The positive mutant fosmid pKLX3, verified by PCR using pairs of primers *H*varf- *H*varr, was first digested by BglII and was then ligated with pHZ1358 to get pKLX4. pKLX4 was isolated and introduced into *S.* by intergeneric conjugation. The double-crossover strain KLX14 was obtained from antibiotic selection (Apr^R) on ISP3 medium (apramycin, 50 mg/ml and nalidixic acid, 50 mg/ml) and was further confirmed by PCR using the pairs of primers *H*varf- *H*varr, respectively.

Gene *30* was amplified with cosmid BAC-AZ1076/33/378 (Kang and Brady, 2014) used as the template. After sequencing, the gene *30* was first recovered as NdeI and EcoRI digestion fragments and was then inserted into the same sites of pET28a (Novagen) leading to recombinant plasmid pKLX5. Plasmid pKLX1 was used as the template for site-directed mutagenesis of arginine 45 (R45) in proteins XanO4. The desired mutations were introduced by Kod-PCR amplification using mutated primers *O4*mutEf-Er, resulting in plasmids pKLX6.

A pJTU1278-derived construct, pKLX7, containing the complete *O4* gene, was used to complement the Δ*O4* mutant ZWK8. pJTU1278 derivative plasmids pKLX8 and pKLX9 carrying intact gene *OVIII* and *30*, respectively, under the control of the *E** promoter, were used for complementation of Δ*O4* mutant. Gene *OVIII* was synthesized by Jieli Biology referring to the original sequence deposited at NCBI (www.ncbi.nlm.nih.gov). All these plasmids were introduced into the Δ*O4* mutant ZWK8 by conjugation, and apramycin- and thiostrepton-resistant (Apr^R, Thio^R) *S.* were selected.

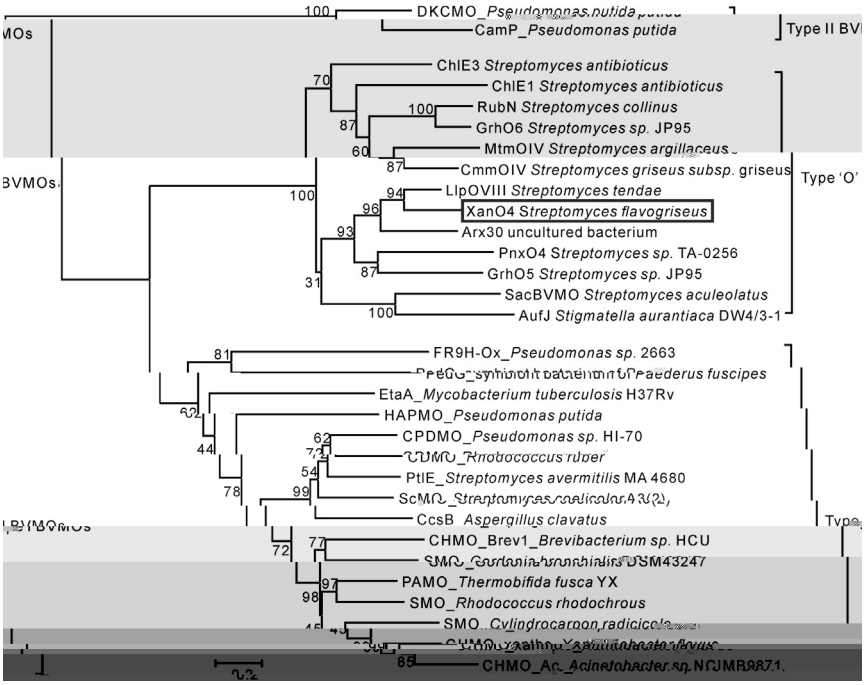

Figure 5. Phylogenetic Analysis of XanO4 with Other Known BVMOs

The neighbor-joining phylogenetic tree was constructed by using MEGA V5.10 with 500 bootstrap replicates. The scale 0.2 is the genetic distance.

Protein Expression and Purification

The expression plasmids for XanO4, Arx30, XanM3, and the site-specific mutagenesis protein XanO4R45A were transformed into *E.* BL21 (DE3)/pLysE, separately. The resultant *E.* BL21 cell was cultured at 37°C and 220 rpm in Luria-Bertani medium supplemented with ampicillin or kanamycin and chloramphenicol (final concentration 100 μg/ml or 50 μg/ml and 25 μg/ml, respectively) to OD_{600} of 0.6. Isopropylthio-β-D-galactoside at a final concentration 0.2 mM was added into the culture after cooling at 4°C for 30 min to induce protein expression. The cells were further cultured at 18°C for 24 hr for XanO4, Arx30, and R45 mutant proteins (as for XanM3, the culture conditions were 30°C for 4–6 hr), and then the cells were harvested by centrifugation (3,500 rpm, 15 min, 4°C) and resuspended in 20 ml of buffer A (50 mM Tris-HCl [pH 8.0], 0.3 M NaCl, and 10% glycerol) and lysed by sonication for 40 min. Cellular debris was removed by centrifugation (12,500 rpm, 60 min, 4°C), and the supernatant was used to purify the protein by nickel-affinity chromatography using standard protocols. The protein was eluted with increasing gradient of buffer B (500 mM imidazole in buffer A). Purified protein was concentrated and exchanged into PBS buffer (50 mM NaH_2PO_4 and Na_2HPO_4 [pH 7.5]) with centrifugal filters (Amicon). The protein was stored in PBS buffer with 10% glycerol at −80°C. Protein concentration was determined with the Bradford assay using BSA as a standard.

Detection of Cofactor Binding by XanO4

To determine the cofactor of XanO4, 80 μM XanO4 was denatured, and the denatured protein was removed by centrifugation. The supernatant retained the distinctive yellow color and was subjected to LC-MS analysis, along with an FAD standard (Sigma-Aldrich) as a positive control.

The LC-MS analysis was conducted on a liquid chromatography-mass spectrometer (Agilent 1100 series LC/MSD Trap system) under positive mode with an Agilent ZORBAX SB-C18 column (5 μm, 4.6 × 250 mm). The column was equilibrated with 95% solvent A (H_2O) and 5% solvent B (acetonitrile) and developed with a linear gradient (5–30 min, from 5% B to 30% B, 30–40 min, from 30% B to 55% B) and then kept in 100% B for 5 min at a flow rate of 0.6 ml/min. The UV irradiation absorbance of cofactor was monitored at 372 nm and 450 nm.

Enzyme Assay

The Duality of Reduced Nicotinamide Nucleotide of XanO4

A 150 μl mixture system containing 50 mM sodium phosphate buffer (pH 7.5), 600 μM NAD(P)H (Sigma-Aldrich), 50 μM **2**, and 15 μM XanO4 was incubated at 30°C. The consumption of reduced nicotinamide nucleotide (NAD(P)H) was assayed by monitoring the variation value at 340 nm using Multiscan Spectrum (BioTek).

In Vitro Assay of XanO4, XanO4R45A, and Arx30

XanO4 (Arx30) activity was assayed by monitoring the conversion of substrate **2** into product **3** as analyzed by LC-MS. A typical 100 μl system consisted of 50 mM sodium phosphate buffer (pH 7.5), 20 μM FAD, 2 mM NAD(P)H, and 50 μM **2**. The reactions were started by adding XanO4 to a final concentration of 20 μM and incubated for 30 min under 30°C. Identical assays with boiled XanO4 (Arx30) were carried out as negative controls.

For time-course analysis of the enzymatic transformation from **2** into **3** catalyzed by XanO4, similar enzymatic reactions were quenched by addition of an equal volume of n-butyl alcohol to precipitate proteins at different time points (0.5 min, 1 min, 2 min, 3 min, and 5 min).

The enzymatic assay system of XanO4R45A was similar to that of XanO4, and reactions were quenched by addition of an equal volume of n-butyl alcohol to precipitate proteins at different time points (0.5 min, 2 hr, 6 hr, 10 hr, and overnight).

Enzyme Assay of XanM3

2 mM **3** and **4** was dissolved in DMSO as stock. A typical reaction system consisted of 80 μM S-adenosyl methionine (AdoMet/SAM; Sigma-Aldrich), 50 μM **3** or **4**, and 20 μM methyltransferase XanM3 in 50 mM potassium phosphate butter (pH 7.5) was used for the conversion of **3** to **5** and **4** to **2**, respectively.

One-Pot Reaction of XanO4 and XanM3

For the one-pot reaction of XanM3 and XanO4 with **2**, 20 μM FAD, 2 mM NADH, 100 μM SAM, and 100 μM **2** were mixed with 20 μM XanO4 and 5 μM XanM3. The reaction mixture was incubated under 30°C for 1 hr.

A similar one-pot reaction of XanM3 and XanO4 with **4** in the presence of 300 μM SAM was conducted as described above.

All the reactions were quenched by the addition of an equal volume of n-BuOH. After extracting three times with n-BuOH, the organic layer was combined and concentrated to dryness, and then finally dissolved in methanol. The methanol extract was analyzed on an Agilent HPLC series 1100 system with an Agilent ZORBAX SB-C18 column (5 μm, 4.6 × 250 mm). The column was equilibrated with 80% solvent A (H_2O) and 20% solvent B (acetonitrile) and developed with a linear gradient (5–35 min, from 20% B to 55% B, 35–40 min, from 55% B to 80% B) and then kept in 100% B for 5 min at a flow rate of 0.6 ml/min and UV detection at 274 nm. LC-MS analysis was conducted with an Agilent 1100 series LC/MSD Trap system with drying gas flow of 10 ml/min, nebulizer at 30 psi, and drying gas temperature of 350°C. For high-resolution mass measurements, an Agilent 1200 series LC/MSD trap system in tandem with a 6530 Accurate-Mass quadrupole time-of-flight (Q-TOF) mass spectrometer was used with an electrospray ionization source (100–1,000 / mass range, negative mode).

Large-Scale Enzymatic Reaction and Purification of Compounds 3 and 4

For the structural elucidation of **3**, the 40 ml reaction system was composed of 20 μM FAD, 500 μM **2**, 50 μM XanO4, and 1 mM NADH in 50 mM PBS (pH 7.5). For compound **4**, the 40 ml reaction system composed of 20 μM FAD, 500 μM **2**, 50 μM XanO4R45A, and 2 mM NADH in 50 mM PBS (pH 7.5) was incubated

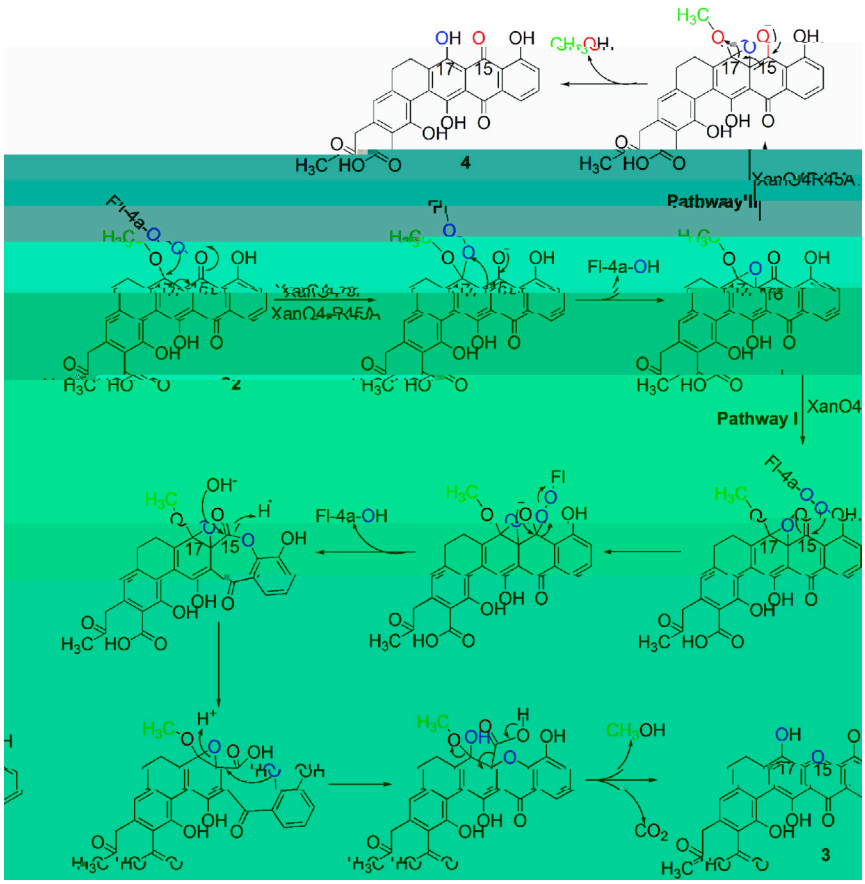

Figure 6. Proposed Enzymatic Mechanisms for XanO4

Red atoms are derived from substrate **2** while blue atoms arise from an oxygen molecule. The green methyl group was disposed from **2** in the form of methanol. The first oxygen insertion catalyzed by XanO4 was proposed to proceed through the attack of activated FAD-O-O^- on carbon atom C17, leading to the formation of a possible anthraquinone epoxide intermediate between carbon C16 and C17. The formation of this anthraquinone epoxide intermediate may facilitate the next nucleophilic attack of FAD-O-O^- on carbonyl carbon atom C15 (in pathway I). Following the classic BV oxidation procedure, the migratory rearrangement led to the formation of a lactone epoxide intermediate. The hydrolysis of lactone initiated the construction of the xanthone ring, opening of the epoxy ring, oxidative decarboxylation, and simultaneous removal of the methoxy group on C17 in the form of methanol. In pathway II, XanO4R45A abolished catalysis of BV oxidation of C15, and somehow produced only demethoxylated anthraquinone **4** via opening of the epoxy ring. The presence of a methoxy group at C17 in **4** prevented the formation of epoxide or recognition by XanO4, so compound **4** existed as a shunt product in the xantholipin biosynthesis pathway.

on a shaker at 160 rpm at 30°C for 4 hr. Then the reaction mixture was extracted three times with an equal volume of n-BuOH, and the organic extract was combined and concentrated to dryness.

The mixture fractionated by DAS-A-HG (120 Å, 50 μm) C18 silica (purchased from H&E Co.) column chromatography with stepwise gradient elution of methanol/water (20%, 30%, 40%, 50%, 70%, 90%, 100%) was then used for further purification, and fractions (40%–70%) containing the target compound were combined. Compounds **3** and **4** were then isolated by semi-preparative HPLC using a C18 column (Thermo Scientific). The column was equilibrated with 70% solvent A (H_2O) and 20% solvent B (acetonitrile) and developed with a linear gradient (0–25 min, from 20% B to 80% B) and then kept in 100% B for 5 min at a flow rate of 2 ml/min with UV detection at 274 nm. ^{1}H-NMR (600 MHz), ^{13}C-NMR (150 MHz), and 2D NMR spectra were recorded using $_6$-DMSO on Bruker Avance III 600 MHz instruments at the instrumental analysis center of Shanghai Jiao Tong University.

Chemical Analysis and Characterization of Compound 5 from *S. flavogriseus* SS101 and *S. flavogriseus* SS101 *ΔxanH* Mutant

Small-scale fermentation cultures of KLX14 mutant were centrifuged at 5,000 rpm for 20 min, and mycelia were extracted with acetone and then concentrated in vacuo. The resulting residue was extracted with ethyl acetate (EtOAc) and concentrated to dryness and finally dissolved in methanol. The methanol extract was analyzed by LC-MS and Q-TOF analysis following the procedure described above.

Large-scale fermentation of KLX14 was conducted according to the standard method described previously. 40 l of fermentation broth was extracted and the organic phase was concentrated leading to 20 g of crude product, which was then fractionated by normal phase silica column chromatography (40–70 μm) with gradient elution of dichloromethane/methanol, and the resultant fractions containing the target compound were combined giving about 100 mg of product. Next DAS-A-HG (120 Å, 50 μm) C18 silica (purchased from H&E Co.) column chromatography with stepwise gradient elution of methanol/water (20%, 30%, 40%, 50%, 70%, 90%, 100%) was then used for further purification, and fractions (40%–70%) containing the target compound were concentrated to give 65 mg of product. Finally, 15 mg of pure **5** was isolated by semi-preparative HPLC using a C18 column (Thermo Scientific). The column was equilibrated with 70% solvent A (H_2O) and 35% solvent B (acetonitrile) and developed with a linear gradient (0–25 min, from 35% B to 100% B) and then kept in 100% B for 5 min at a flow rate of 2 ml/min with UV detection at 274 nm. ^{1}H-NMR (600 MHz), ^{13}C-NMR (150 MHz), and 2D NMR spectra were recorded using $_6$-DMSO on Bruker Avance III 600 MHz instruments at the instrumental analysis center of Shanghai Jiao Tong University.

Detection of the Possible Leaving Group of C17 during the Conversion of 2 to 3

For MS detection of the possible formaldehyde-bisulfite adduct $CH_2(OH)SO_3^-$ (HMS^-, / = 111) formed in the XanO4 catalyzed reaction, 2 mM bisulfite was added into the reaction system. After incubation for 1 hr at 30°C, an equal volume of ethyl acetate was added for the disposal of protein, and the water phase was concentrated to minimal volume. Then the reaction liquid was detected using an LC-MS system under negative ion mode with standard HMS as positive control.

A positive reaction system of 20 μl of formaldehyde with 2 mM bisulfate in 50 mM PBS buffer was incubated for 1 hr at 30°C. The reaction system was concentrated into minimal volume before LC-MS analysis with an Agilent ZORBAX SB-C18 column (5 μm, 4.6 × 250 mm). The column was equilibrated with 80% solvent A (10 mM NH_4AC) and 20% solvent B (acetonitrile) and developed with a linear gradient (5–30 min, from 20% B to 50% B, 35–40 min, from 50% B to 100% B) and then kept in 100% B for 5 min at a flow rate of 0.6 ml/min.

Detection of the Origin of Oxygen at C17 in 3 and 4 with H_2O^{18} and $^{18}O_2$

To test the origin of oxygen at C17 in **3**, a typical 100 μl closed enzymatic assay system composed of 20 μM XanO4, 20 μM FAD, 2 mM NADH, and

100 μM **2** was incubated under $^{18}O_2$. As for the production of compound **4**, 20 μM XanO4R45A was used instead. The $^{16}O_2$ in the reaction system was replaced with N_2 before the filling of $^{18}O_2$. The reaction was initiated by the addition of XanO4 or XanO4R45A. After incubation for 2 hr, the reaction system was extracted twice with an equal volume of n-BuOH. The organic extract was combined and concentrated to dryness before detection by HPLC-MS.

Another enzymatic assay system was composed of 20 μM XanO4, 20 μM FAD, 1 mM NADH, and 100 μM **2** dissolved in H_2O^{18} with 50 mM Na_2HPO_4/NaH_2PO_4. The reaction was initiated by the addition of XanO4. After incubation for 30 min, the reaction system was extracted following the method described above and was analyzed by LC-MS.

Phylogenetic Analysis

Detailed information is given in Supplemental Experimental Procedures.

ACCESSION NUMBERS

The accession number for XanO4 is Genbank: ADE22300.1 and ADE22301.1 for XanM3. The accession number for Arx30 is Genbank: AHX24715.1. The accession number for LlpOVIII is Genbank: CAM34363.1.

SUPPLEMENTAL INFORMATION

Supplemental Information includes Supplemental Experimental Procedures, six figures, and three tables and can be found with this article online at http://dx.doi.org/10.1016/j.chembiol.2016.03.013.

AUTHOR CONTRIBUTIONS

L.X.K. and D.L.Y. designed the study. L.X.K., W.K.Z., and L.W. performed all the experiments. L.X.K., W.K.Z., Y.H.C., B.C., and D.L.Y. analyzed the results. L.X.K. and D.L.Y. wrote the paper.

ACKNOWLEDGMENTS

This work was supported by grants from the National Natural Science Foundation of China (31170085, 31470183, 30771174, 30670032, and 31070058); the Ministry of Science and Technology (2012CB721004, 2006AA02Z224, and 2009ZX09501-008); Shanghai Pujiang Program from the Shanghai Municipal Council of Science and Technology (12PJD021). We thank Sean F. Brady at the Rockefeller University for providing the cosmid BAC-AZ1076/33/378 for cloning and enzymatic characterization of Arx30. We thank Prof. Gongli Tang and Shuangjun Lin for supporting the isotope labeling experiment. We also thank Nelson Lloyd Brock and Xiaozheng Wang for the NMR analysis.

Received: February 19, 2016
Revised: February 19, 2016
Accepted: March 17, 2016
Published: April 21, 2016

REFERENCES

Bailey, W.F., and Bischoff, J.J. (1985). Formation of cyclic ethers in the double Baeyer-Villiger oxidation of ketals derived from cyclic ketones. J. Org. Chem. *50*, 3009–3010.

Bailey, W.F., and Shih, M.-J. (1982). Oxidation of ketals to orthocarbonates: a double Baeyer-Villiger reaction. J. Am. Chem. Soc. *104*, 1769–1771.

Beam, M.P., Bosserman, M.A., Noinaj, N., Wehenkel, M., and Rohr, J. (2009). Crystal structure of Baeyer-Villiger monooxygenase MtmOIV, the key enzyme of the mithramycin biosynthetic pathway. Biochemistry *48*, 4476–4487.

Berkel, W.J.H.V., Kamerbeek, N.M., and Fraaije, M.W. (2006). Flavoprotein monooxygenases, a diverse class of oxidative biocatalysts. J. Biotechnol. *124*, 670–689.

Bockholt, H., Udvarnoki, G., Rohr, J., Mocek, U., Beale, J.M., and Floss, H.G. (1994). Biosynthetic studies on the xanthone antibiotics lysolipins X and I. J. Org. Chem. *59*, 2064–2069.

Butler, J.R., Wang, C., Bian, J., and Ready, J.M. (2011). Enantioselective total synthesis of (−)-kibdelone C. J. Am. Chem. Soc. *133*, 9956–9959.

Carter, G.T., Goodman, J.J., Torrey, M.J., Borders, D.B., and Gould, S.J. (1989). Biosynthetic origin of the carbon skeleton of simaomicin alpha, a hexacyclic xanthone antibiotic. J. Org. Chem. *54*, 4321–4323.

Carter, G.T., Borders, D.B., Goodman, J.J., Ashcroft, J., Greenstein, M., Maiese, W.M., and Pearce, C.J. (1991). Biosynthetic origins of the polycyclic xanthone antibiotic, citreamicin. J. Chem. Soc. Perkin Trans. 1, 2215–2219.

Datsenko, K.A., and Wanner, B.L. (2000). One-step inactivation of chromosomal genes in *E* K-12 using PCR products. Proc. Natl. Acad. Sci. USA *97*, 6640–6645.

Gibson, M., Nur-e-alam, M., Lipata, F., Oliveira, M.A., and Rohr, J. (2005). Characterization of kinetics and products of the Baeyer-Villiger oxygenase MtmOIV, the key enzyme of the biosynthetic pathway toward the natural product anticancer drug mithramycin from *S* . J. Am. Chem. Soc. *127*, 17594–17595.

Gust, B., Challis, G.L., Fowler, K., Kieser, T., and Chater, K.F. (2003). PCR-targeted *S* gene replacement identifies a protein domain needed for biosynthesis of the sesquiterpene soil odor geosmin. Proc. Natl. Acad. Sci. USA *100*, 1541–1546.

He, Y., Wang, Z., Bai, L., Liang, J., Zhou, X., and Deng, Z. (2010). Two pHZ1358-derivative vectors for efficient gene knockout in streptomyces. J. Microbiol. Biotechnol. *20*, 678–682.

Henry, K.M., and Townsend, C.A. (2005). Ordering the reductive and cytochrome P450 Oxidative steps in demethylsterigmatocystin formation yields general insights into the biosynthesis of aflatoxin and related fungal metabolites. J. Am. Chem. Soc. *127*, 3724–3733.

Hu, Y., Dietrich, D., Xu, W., Patel, A., Thuss, J.A., Wang, J., Yin, W.B., Qiao, K., Houk, K.N., Vederas, J.C., et al. (2014). A carbonate-forming Baeyer-Villiger monooxygenase. Nat. Chem. Biol. *10*, 552–554.

Jiang, J., Tetzlaff, C.N., Takamatsu, S., Iwatsuki, M., Komatsu, M., Ikeda, H., and Cane, D.E. (2009). Genome mining in *S* : a biochemical Baeyer-Villiger reaction and discovery of a new branch of the pentalenolactone family tree. Biochemistry *48*, 6431–6440.

Jiang, W., Wilson, M.A., and Weeks, D.P. (2013). O-Demethylations catalyzed by Rieske nonheme iron monooxygenases involve the difficult oxidation of a saturated C-H bond. ACS Chem. Biol. *8*, 1687–1691.

Kang, H.-S., and Brady, S.F. (2014). Arixanthomycins A-C: phylogeny-guided discovery of biologically active eDNA-derived pentangular polyphenols. ACS Chem. Biol. *9*, 1267–1272.

Kelly, T.R., Jagoe, C.T., and Li, Q. (1989). Synthesis of (.+-.) cervinomycins A1 and A2. J. Am. Chem. Soc. *111*, 4522–4524.

Kieser, T., Bibb, M.J., Buttner, M.J., Chater, K.F., and Hopwood, D.A. (2000). Practical Streptomyces Genetics (John Innes Foundation).

Klose, R.J., Kallin, E.M., and Zhang, Y. (2006). JmjC-domain-containing proteins and histone demethylation. Nat. Rev. Genet. *7*, 715–727.

Knueppel, D., Yang, J., Cheng, B., Mans, D., and Martin, S.F. (2015). Total synthesis of the aglycone of IB-00208. Tetrahedron *71*, 5741–5757.

Kondo, K., Eguchi, T., Kakinuma, K., Mizoue, K., and Qiao, Y.F. (1998). Structure and biosynthesis of FD-594; a new antitumor antibiotic. J. Antibiot. *51*, 288–295.

Kudo, F., Yonezawa, T., Komatsubara, A., Mizoue, K., and Eguchi, T. (2011). Cloning of the biosynthetic gene cluster for naphthoxanthene antibiotic FD-594 from *S* sp. TA-0256. J. Antibiot. *64*, 123–132.

Leisch, H., Morley, K., and Lau, P.C.K. (2011). Baeyer-Villiger monooxygenases: more than just green chemistry. Chem. Rev. *111*, 4165–4222.

Lopez, P., Hornung, A., Welzel, K., Unsin, C., Wohlleben, W., Weber, T., and Pelzerb, S. (2010). Isolation of the lysolipin gene cluster of *S* - Tü 4042. Gene *461*, 5–14.

Masters, K.S., and Bräse, S. (2012). Xanthones from fungi, lichens, and bacteria: the natural products and their synthesis. Chem. Rev. *112*, 3717–3776.

Masuo, R., Ohmori, K., Hintermann, L., Yoshida, S., and Suzuki, K. (2009). First stereoselective total synthesis of FD-594 aglycon. Angew. Chem. Int. Ed. Engl. *48*, 3462–3465.

Paget, M.S., Chamberlin, L., Atrih, A., Foster, S.J., and Buttner, M.J. (1999). Evidence that the extracytoplasmic function sigma factor sigmaE is required for normal cell wall structure in *S* A3(2). J. Bacteriol. *181*, 204–211.

Pinto, M.M., Sousa, M.E., and Nascimento, M.S. (2005). Xanthone derivatives: new insights in biological activities. Curr. Med. Chem. *12*, 2517–2538.

Sambrook, J., and Russel, D.W. (2001). Molecular Cloning: A Laboratory Manual (Cold Spring Harbor Laboratory Press).

Sloman, D.L., Bacon, J.W., and Porco, J.A. (2011). Total synthesis and absolute stereochemical assignment of kibdelone C. J. Am. Chem. Soc. *133*, 9952–9955.

Suginome, H., and Yamada, S. (1984). Replacement of a carbonyl group of cyclic ketones by an oxygen atom: a four-step transformation of cyclic ketones into cyclic ethers. Tetrahedron Lett. *25*, 3995–3998.

Suginome, H., and Yamada, S. (1985). Replacement of a carbonyl group of camphor by an oxygen atom. Synthesis of 1,7,7-trimethyl-2-oxabicyclo (2.2.1)heptane. Bull. Chem. Soc. Jpn. *58*, 3055–3056.

Tang, M.C., He, H.Y., Zhang, F., and Tang, G.L. (2013). Baeyer-Villiger oxidation of acyl carrier protein-tethered thioester to acyl carrier protein-linked thiocarbonate catalyzed by a monooxygenase domain in FR901464 biosynthesis. ACS Catal. *3*, 444–447.

Terui, Y., Yiwen, C., Jun-ying, L., Ando, T., Yamamoto, H., Kawamura, Y., Tomishima, Y., Uchida, S., Okazaki, T., Munetomo, E., et al. (2003). Xantholipin, a novel Inhibitor of HSP47 gene expression produced by *S* sp. Tetrahedron Lett. *34*, 5427–5430.

Walker, E.R., Leung, S.Y., and Barrett, A.G.M. (2005). Studies towards the total synthesis of Sch 56036; isoquinolinone synthesis and the synthesis of phenanthrenes. Tetrahedron Lett. *46*, 6537–6540.

Winter, D.K., Sloman, D.L., and Porco, J.A. (2013). Polycyclic xanthone natural products: structure, biological activity and chemical synthesis. Nat. Prod. Rep. *30*, 382–391.

Yang, J., Knueppel, D., Cheng, B., Mans, D., and Martin, S.F. (2015). Approaches to polycyclic 1,4-dioxygenated xanthones. Application to total synthesis of the aglycone of IB-00208. Org. Lett. *17*, 114–117.

Yunt, Z., Reinhardt, K., Li, A., Engeser, M., Dahse, H.M., Gütschow, M., Bruhn, T., Bringmann, G., and Piel, J. (2009). Cleavage of four carbon-carbon bonds during biosynthesis of the griseorhodin a spiroketal pharmacophore. J. Am. Chem. Soc. *131*, 2297–2305.

Zhang, W.K., Wang, L., Kong, L.X., Wang, T., Chu, Y., Deng, Z.X., and You, D.L. (2012). Unveiling the post-PKS redox tailoring steps in biosynthesis of the Type II polyketide antitumor antibiotic xantholipin. Chem. Biol. *19*, 422–432.